Thermal lattice Boltzmann method based on a theoretically simple derivation of the Taylor expansion

Jae Wan Shim*

Interdisciplinary Fusion Technology Division, KIST and the University of Science and Technology, 136-791, Seoul, Republic of Korea,

Renée Gatignol

Institut Jean le Rond d'Alembert, Université Pierre et Marie Curie and CNRS, 4 Place Jussieu, 75252 Paris cedex 05, France

(Received 28 October 2009; published 25 April 2011; publisher error corrected 3 May 2011)

We propose an approach to derive the thermal lattice Boltzmann method that is based on the Taylor expansion in variables of *temperature as well as velocity* and a direct calculation upon the Gaussian quadrature based hypothesis. This enables us to overcome the isothermal limitation and the low-order accuracy simultaneously. A systematic framework is explained for constructing numerically stable lattice Boltzmann models. The stability of this one-dimensional lattice Boltzmann model is demonstrated with a shock tube simulation.

DOI: 10.1103/PhysRevE.83.046710 PACS number(s): 05.20.Dd, 47.11.−j, 47.10.−g

I. INTRODUCTION

Fluids can be simulated by various methods based on the governing equations such as the Euler, the Navier-Stokes, and the Boltzmann equations. The continuum hypothesis is needed to use the Navier-Stokes equations for a liquid or for a not too rarefied gas. However, a rarefied gas violates the continuum hypothesis. In this case, we can simulate it by considering the Boltzmann equation, which describes the distribution of a single particle in a fluid with respect to phase space and time. In addition, for a not too rarefied gas, we can obtain the Euler equations or the Navier-Stokes equations from the Boltzmann equation by the Chapman-Enskog expansion, which is an approximation procedure. The classical shock tube problem is one of the famous problems in the continuum regime and it can be solved by use of the Euler equations.

The lattice Boltzmann method (LBM) was originally developed from lattice gas cellular automata and later it was recognized that the LBM can be obtained by discretization of the Boltzmann equation with the Bhatnagar-Gross-Krook (BGK) collision term [1]. Therefore, the LBM is a solver for the Navier-Stokes equations and, in addition, can solve for the flows in the rarefied gas regime. The isothermal LBM is well established at a low Mach number and from it we can recover the Navier-Stokes equations [2–4]. Recently, Chikatamarla and Karlin [5,6] developed a theory of isothermal lattice Boltzmann models based on the relation between entropy construction and the roots of Hermite polynomials.

The thermal LBM (TLBM) was developed from the isothermal LBM by including thermal effects. There are two major approaches, the multispeed [7–9] and the double-population one [10]. These methods have problems such as numerical instability, a limited temperature variation, and their unavailability for compressible flows. A recently proposed TLBM [11], based on a so-called consistent LBM [12], is applicable to simulation of thermal flows. Shan *et al.* presented an interesting framework in which to derive the TLBM using Hermite polynomials and the Hermite-Gauss quadrature [13]. They provided some models applicable to regular lattices without using the Hermite-Gauss quadrature. However, their systematic formulation procedure does not provide a higher-order model having rational number ratios between different amplitudes of nonzero discrete velocities because their ratios have those of the Hermite-Gauss quadrature abscissas. This fact prohibits the possibility of using regular lattices. The work of Philippi *et al.* [14] and Siebert *et al.* [15] uses the Taylor expansion in terms of temperature to obtain the TLBM. In fact, they use a mixture of the Taylor expansion and the Hermite expansion for the temperature and the velocity, respectively. Therefore, their derivation is complicated. Their framework is different from ours which will be presented. We use the symbol D for D-dimensional space for our equilibrium distribution; however, Philippi *et al.* restricted their final development of the equilibrium distribution to two-dimensional space. In the specific case of $D = 2$, some terms are common but their result is more similar to the Hermite expansion.

In this paper, we propose a theoretically simple approach to derive the isothermal lattice Boltzmann models obtained by Chikatamarla and Karlin. Moreover, we show that our framework easily gives the thermal lattice Boltzmann models. With use of this TLBM, we show a simulation of a shock tube problem to illustrate the stability of our model.

The Boltzmann equation can be written as Eq. (1) with use of the BGK collision term and the assumption of no external force:

$$\partial_t f + \mathbf{V} \cdot \nabla f = -(f - f^{eq})/\tau. \tag{1}$$

The infinitesimal quantity $f d\mathbf{x} d\mathbf{V}$ is the number of particles having velocity $\mathbf{V}$ in an infinitesimal element of phase space $d\mathbf{x} d\mathbf{V}$ at position $\mathbf{x}$ at time t. The symbol τ, a constant relaxation time, adjusts the attitude to approach the Maxwell-Boltzmann (MB) distribution f^{eq} due to collision. The macroscopic physical properties are obtained from

$$n = \int f d\mathbf{V}, \tag{2}$$

$$n\mathbf{U} = \int \mathbf{V} f d\mathbf{V}, \tag{3}$$

$$2ne = \int \|\mathbf{V} - \mathbf{U}\|^2 f d\mathbf{V}, \tag{4}$$

*Corresponding author: jae-wan.shim@polytechnique.org

where n is the number density, $\mathbf{U}$ is the macroscopic velocity, and e is the energy per unit of mass. We can relate e to the temperature by $e = DkT/(2m)$ where D is the dimension of space, k is the Boltzmann constant, T is the temperature, and m is the molecular mass. The MB distribution is

$$f^{eq} = n(\pi\,\Theta)^{-D/2}\exp(-\|\mathbf{V}-\mathbf{U}\|^2/\Theta), \tag{5}$$

where Θ is defined by $\Theta = 2kT/m = 4e/D$, and where n, $\mathbf{U}$, and Θ satisfy Eqs. (2), (3), and (4).

The LBM is the discretized version of Eq. (1) in phase space and time. We can obtain the time discretization which is done in the paper [16]. The essential work of the discretization is to find the discretized f^{eq}, on which we will now focus.

II. DISCRETIZATION OF THE EQUILIBRIUM DISTRIBUTION

We use a lightface type for the amplitude of a vector expressed by a boldface symbol. The second-order Taylor expansion (TE) of Eq. (5) with respect to $\mathbf{U} = \mathbf{U_0} = \mathbf{0}$ and $\Theta = \Theta_0$ in D-dimensional space is

$$f^{eq(2)}_{TE} = n(\pi\,\Theta_0)^{-D/2}\exp(-v^2)[\psi+\varphi], \tag{6}$$

where

$$\psi = 1 + 2\mathbf{v}\cdot\mathbf{u} + 2(\mathbf{v}\cdot\mathbf{u})^2 - u^2 \tag{7}$$

and

$$\varphi = \underbrace{\sigma(-D/2+v^2)}_{\varphi_1} + \underbrace{\sigma[-(2+D)+2v^2](\mathbf{v}\cdot\mathbf{u})}_{\varphi_2} + \underbrace{\sigma^2[(2D+D^2)/4-(2+D)v^2+v^4]/2}_{\varphi_3}. \tag{8}$$

Note that $\mathbf{v} = \mathbf{V}/\sqrt{\Theta_0}$, $\mathbf{u} = \mathbf{U}/\sqrt{\Theta_0}$, $\sigma = \theta - 1$, and $\theta = \Theta/\Theta_0$, and we omit the Lagrange remainder for the TE in Eq. (6). We emphasize that $f^{eq(2)}_{TE}$ satisfies Eqs. (2), (3), and (4). In addition, it is important to remark that $\mathbf{u}$ and σ are infinitely small quantities of the same order.

If the infinitely small quantities $\mathbf{u}$ and $\sqrt{|\sigma|}$ are taken as the same order instead of the previous choice, we obtain the result obtained by Shan *et al.* using the Hermite expansion and Hermite-Gauss quadrature [13]. They obtained the second- and the third-order Hermite expansions, respectively, $f^{eq(2)}_{HE} = \lambda[\psi+\varphi_1]$ and $f^{eq(3)}_{HE} = \lambda[\psi + 4(\mathbf{v}\cdot\mathbf{u})^3/3 - 2u^2(\mathbf{v}\cdot\mathbf{u}) + \varphi_1 + \varphi_2]$, where $\lambda = n(\pi\,\Theta_0)^{-D/2}\exp(-v^2)$, and φ_1 and φ_2 are indicated in Eq. (8). The second-order Hermite expansion (HE) does not possess φ_2 and φ_3 of Eq. (8). For the case of the third-order HE, the third-order term of $\mathbf{u}$ appears in ψ; however, φ_3 disappears. The expansions following the Hermite polynomials are obtained by selecting $\mathbf{v}$ as an expansion variable. We realized that the HEs correspond to the TEs with the infinitely small quantities $\mathbf{u}$ and $\sqrt{|\sigma|}$ of the same order.

Let f_i^{eq} be a discrete f^{eq}_{TE} with respect to $\mathbf{v}$ defined by

$$f_i^{eq}(\mathbf{v}_i) = W_i\lambda(\mathbf{v}_i)\{\psi(\mathbf{v}_i)+\varphi(\mathbf{v}_i)\}, \tag{9}$$

where W_i or p_i defined by $p_i = W_i\,\lambda(\mathbf{v}_i)/n$ for simplicity is a weighting coefficient. We expressed the argument $\mathbf{v}_i$ to emphasize the discretization with respect to $\mathbf{v}$ in Eq. (9). We want to find W_i which satisfies $\theta_0^{D/2}\int P(\mathbf{v})f^{eq}(\mathbf{v})\,d\mathbf{v} = \sum_i P(\mathbf{v}_i)f_i^{eq}(\mathbf{v}_i)$, where $P(\mathbf{v})$ is a polynomial in variables of the components of $\mathbf{v}$. Note that $\Theta_0^{D/2}d\mathbf{v} = d\mathbf{V}$; therefore, we use $d\mathbf{V}$ for simplicity. We neglect the TE error, i.e., the Lagrange remainder, so we have

$$\int P(\mathbf{v})f^{eq}_{TE}(\mathbf{v})\,d\mathbf{V} = \sum_i P(\mathbf{v}_i)f_i^{eq}(\mathbf{v}_i). \tag{10}$$

When $P(\mathbf{v}) = 1$, $\mathbf{v}$, and $\|\mathbf{v}-\mathbf{u}\|^2$, if we apply Eq. (10), we get the constraints

$$n = \int f^{eq}_{TE}(\mathbf{v})\,d\mathbf{V} = \sum_i f_i^{eq}(\mathbf{v}_i), \tag{11}$$

$$n\mathbf{u} = \int \mathbf{v}\,f^{eq}_{TE}(\mathbf{v})\,d\mathbf{V} = \sum_i \mathbf{v}_i\,f_i^{eq}(\mathbf{v}_i), \tag{12}$$

$$\frac{Dn\theta}{2} = \int \|\mathbf{v}-\mathbf{u}\|^2 f^{eq}_{TE}(\mathbf{v})\,d\mathbf{V} = \sum_i \|\mathbf{v}_i-\mathbf{u}\|^2 f_i^{eq}(\mathbf{v}_i). \tag{13}$$

Note that the values n, $n\mathbf{u}$, and $Dn\theta/2$ are calculated directly from the integral of the MB distribution. Equations (11), (12), and (13) define the satisfaction of the equalities of mass, momentum, and energy between the continuous and discrete velocity fields, respectively.

We find $f_i^{eq}(\mathbf{v}_i)$ which satisfies the constraints of Eqs. (11), (12), and (13) for one-dimensional space. The vector $\mathbf{v}_i$ becomes a scalar v_i and we let $v_i = r_i$. We define the hypothesis

$$\int_{-\infty}^{\infty} e^{-r^2}P(r)dr = \sum_{\alpha=1}^{k} w_\alpha P(r_\alpha). \tag{14}$$

We define $\sum w_\alpha r_\alpha^d = \Xi(d)$. If we apply the hypothesis on Eqs. (11), (12), and (13), we obtain seven equations that we present in two groups, G_I and G_{II},

$$\begin{aligned} G_I:&\ \begin{cases}\Xi(0)=\sqrt{\pi}, & \Xi(1)=0, \quad \Xi(2)=\sqrt{\pi}/2,\\ \Xi(3)=0, & \Xi(4)=3\sqrt{\pi}/4, \quad \Xi(5)=0,\end{cases}\\ G_{II}:&\ \Xi(6)=15\sqrt{\pi}/8.\end{aligned} \tag{15}$$

Note that the G_{II} in Eq. (15) is obtained because of the second -order term in σ of Eq. (8), which is different from the third-order HE of Shan *et al.* According to the Hermite-Gauss quadrature [17] with $k = 3$ of Eq. (14), we can obtain $r_1 = 0$, $r_{2,3} = \pm\sqrt{6}/2$, and $w_1 = 2\sqrt{\pi}/3$, $w_{2,3} = \sqrt{\pi}/6$. These solutions are identical to the solutions of obly the G_I of Eq. (15). Therefore, we try to find the solutions of Eq. (14) for the regular lattice geometry with $k = 5$ using G_I, G_{II}, and the symmetry conditions $\{r_1 = 0,\ r_2 = -r_3,\ r_4 = -r_5,\ r_4/r_2 = p/q\}$ where p and q are relatively prime. Note that the case of $k = 5$ gives the five-velocity model while the case of $k = 3$ gives the three-velocity model. When $p = 2$ and $q = 1$, there is no solution. When $p = 3$ and $q = 1$, we have two solution sets, S_I and S_{II},

$$\begin{aligned} S_I: r_1 &= 0, \quad w_1 = 4(4-\sqrt{10})\sqrt{\pi}/45,\\ r_{2,3} &= \pm\sqrt{(5-\sqrt{10})/6}, \quad w_{2,3} = 3(8+\sqrt{10})\sqrt{\pi}/80,\\ r_{4,5} &= \pm 3r_2, \quad w_{4,5} = (16+5\sqrt{10})\sqrt{\pi}/720.\end{aligned} \tag{16}$$

$$S_{II}:\ r_1 = 0,\quad w_1 = 4(4+\sqrt{10})\sqrt{\pi}/45,$$
$$r_{2,3} = \pm\sqrt{(5+\sqrt{10})/6},\quad w_{2,3} = 3(8-\sqrt{10})\sqrt{\pi}/80, \tag{17}$$
$$r_{4,5} = \pm 3r_2,\quad w_{4,5} = (16-5\sqrt{10})\sqrt{\pi}/720.$$

Note that the solution S_{II} is similar to the solution of the Hermite-Gauss quadrature with $k = 3$ because of the small values of w_4 and w_5. Chikatamarla and Karlin found the solution S_{II} in Eq. (16) of their paper [6]; however, they could show an *isothermal* shock tube simulation. Eventually, with the solution S_I of Eq. (16), we can construct the one-dimensional five-velocity model by use of $f_i^{eq}(v_i) = (nw_i/\sqrt{\pi})\{\psi(v_i)+\varphi(v_i)\}$.

Henceforth, we find two-dimensional hexagonal models. We introduce polar coordinates for convenience to deal with the hexagonal model. Let $\mathbf{v} = (r\cos\phi, r\sin\phi)$ and $\mathbf{u} = (u\cos\delta, u\sin\delta)$. Then we have

$$\int P(\mathbf{v}) f_{TE}^{eq}(\mathbf{v}) d\mathbf{V} = \frac{n}{\pi}\int_0^{2\pi}\int_0^{\infty} Pe^{-r^2}\{\psi+\varphi\} r dr d\phi, \tag{18}$$

where $P = P(r,\phi)$, $\psi = \psi(u,\delta,r,\phi)$, and $\phi = \phi(\theta,u,\delta,r,\phi)$ [18]. We define the hypothesis

$$\int_0^{\infty} re^{-r^2}P(r)dr = \sum_{\alpha=0}^{k} w_\alpha P(r_\alpha) \tag{19}$$

where $r_0 = 0$. This hypothesis is similar to the Laguerre quadrature [17] but not the same. Our objective is to find w_α and r_α. We apply this hypothesis, i.e., Eq. (19), to Eq. (18). Then

$$\int P(\mathbf{v}) f_{TE}^{eq}(\mathbf{v}) d\mathbf{V} = \frac{n}{\pi}\sum_{\alpha=0}^{k} w_\alpha \int_0^{2\pi} P(r_\alpha)\{\psi(r_\alpha)+\varphi(r_\alpha)\} d\phi. \tag{20}$$

We calculate the right-hand side integral of Eq. (20) when $P(\mathbf{v}) = 1$, $\mathbf{v}$, and $\|\mathbf{v}-\mathbf{u}\|^2$. Then we compare the results with Eqs. (11), (12), and (13), respectively. Consequently, we obtain a system of equations which satisfy simultaneously Eqs. (11), (12), and (13),

$$\sum w_\alpha = 1/2,\quad \sum w_\alpha r_\alpha^2 = 1/2,$$
$$\sum w_\alpha r_\alpha^4 = 1, \text{ and } \sum w_\alpha r_\alpha^6 = 3. \tag{21}$$

Note that if we calculate Eq. (20) for $P(\mathbf{v}) = v^2\mathbf{v}$ and $P(\mathbf{v}) = \|\mathbf{v}-\mathbf{u}\|^4$, respectively, we have the equation sets $\{\sum w_\alpha r_\alpha^4 = 1,\ \sum w_\alpha r_\alpha^6 = 3\}$ and $\sum w_\alpha r_\alpha^8 = 12$. The former is consistent with Eq. (21) but the latter is a spurious constraint from the point of view of physical property conservation. This also means that the solution sets of Eq. (21) satisfy the third momentum of $\mathbf{v}$.

We can achieve the discretization of ϕ by

$$\int_0^{2\pi}\cos^n\phi\ \sin^m\phi\ d\phi = \frac{\pi}{3}\sum_{\beta=1}^{6}\cos^n\left(\frac{\beta\pi}{3}\right)\sin^m\left(\frac{\beta\pi}{3}\right), \tag{22}$$

where $n+m \leqslant 5$ and n,m are zero or natural numbers. It is easy to verify this identity by direct calculations for each case of n and m. Therefore, we can rewrite Eq. (20) as

$$\int P(\mathbf{v}) f_{TE}^{eq}(\mathbf{v}) d\mathbf{V} = \frac{n}{3}\sum_{\alpha=0}^{k}\sum_{\beta=1}^{6} w_\alpha P(r_\alpha,\phi_\beta)\{\psi(r_\alpha,\phi_\beta)+\varphi(r_\alpha,\phi_\beta)\} \tag{23}$$

where $\phi_\beta = \beta\pi/3$. Note that the limitation of $n+m \leqslant 5$ is sufficient up to the case of $P(\mathbf{v}) = \|\mathbf{v}-\mathbf{u}\|^4$.

We define the discrete 13 velocities by

$$\mathbf{v}_i = \begin{cases} (0,0) & \text{for } i = 0,\\ c(\cos(\pi i/3), \sin(\pi i/3)) & \text{for } i = 1 \text{ to } 6,\\ 2c(\cos(\pi i/3), \sin(\pi i/3)) & \text{for } i = 7 \text{ to } 12,\end{cases} \tag{24}$$

where c is a constant determined later. Equation (23) with $k = 2$ matches the 13-velocity model if we put $r_0 = 0$, $r_1 = c$, and $r_2 = 2c$ with which we can solve Eq. (21). We have two solution sets, S_I and S_{II},

$$S_I:\ w_0 = 1/8,\quad w_1 = 1/3,\quad w_2 = 1/24,\quad c = 1, \tag{25}$$

$$S_{II}:\ w_0 = 7/36,\quad w_1 = 8/27,\quad w_2 = 1/108,\quad c = \sqrt{3/2}. \tag{26}$$

From Eq. (23) with Eqs. (25) and (26), we finally obtain the discrete MB distributions $f_i^{eq}(\mathbf{v}_i) = np_i\{\psi(\mathbf{v}_i)+\varphi(\mathbf{v}_i)\}$ with Eq. (24) and

$$p_i = \begin{cases} 1/4 & \text{for } i = 0,\\ 1/9 & \text{for } i = 1 \text{ to } 6,\\ 1/72 & \text{for } i = 7 \text{ to } 12,\end{cases} \quad \text{with } c = 1 \tag{27}$$

or

$$p_i = \begin{cases} 7/18 & \text{for } i = 0,\\ 8/81 & \text{for } i = 1 \text{ to } 6,\\ 1/324 & \text{for } i = 7 \text{ to } 12,\end{cases} \quad \text{with } c = \sqrt{\frac{3}{2}}. \tag{28}$$

Note that the values of p_i are obtained from Eqs. (11), (12), and (13) and can be easily obtained from the solution sets (25) and (26) after the normalization of w_i while considering the number of discrete velocities having the same amplitudes. It is emphasized again that Eqs. (27) and (28) satisfy $\sum f_i^{eq}(\mathbf{v}_i) = n$, $\sum \mathbf{v}_i f_i^{eq}(\mathbf{v}_i) = n\,\mathbf{u}$, and $\sum \|\mathbf{v}_i - \mathbf{u}\|^2 f_i^{eq}(\mathbf{v}_i) = n\,\theta$. These 13-velocity models can be used for the thermal lattice Boltzmann method. The advantage is that we can choose θ_0 to obtain a better approximation. Note that the two-dimensional, hexagonal, 19-velocity model was also studied in this framework [18]. In addition, these 13- and 19-velocity models were used to simulate microchannel isothermal and thermal flows [18,19]. Pavlo *et al.* wrote in their paper [20] that the hexagonal lattice exhibits better stability properties than the square lattice, but it does not exhibit sufficient isotropy to eliminate the spurious cubic deviations in the macroscopic conservation equations. And they suggested octagonal models which are not applicable to regular lattices.

III. SIMULATION RESULT

We show in Fig. 1 the simulation result of the one-dimensional shock tube problem performed using the

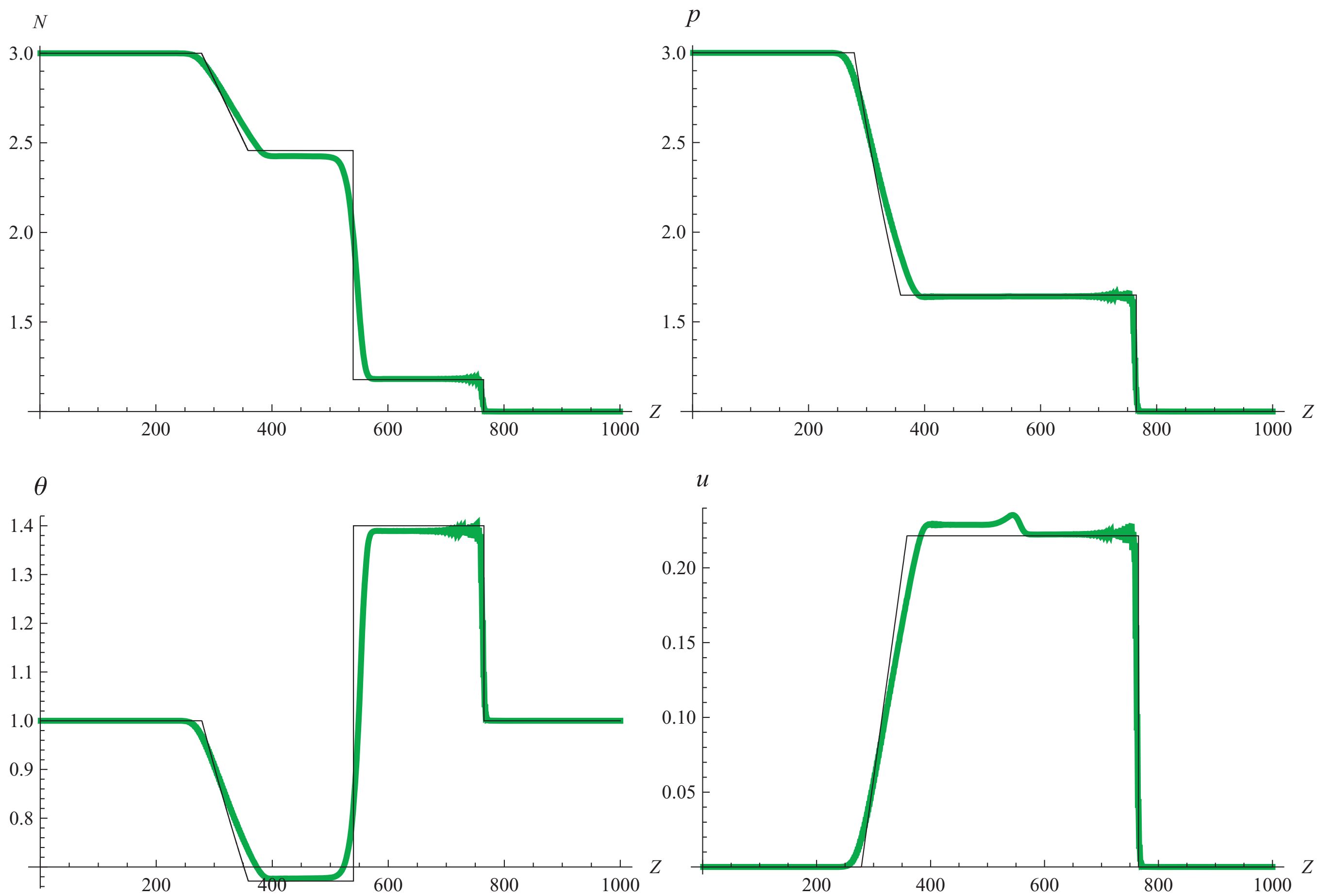

FIG. 1. (Color online) Simulation results of the one-dimensional shock tube problem by our one-dimensional five-velocity model (thick green line) and the analytical solution of the Riemann problem (thin black line) after 100 time steps. The vertical axis labels N, p, θ, and u represent the normalized density, pressure, temperature, and velocity, respectively. The horizontal axis label Z represents the location number.

one-dimensional five-velocity model of our framework, precisely the solution S_I of Eq. (16), and we compare it with the analytical solution of the Riemann problem. It is important to notice that our framework provides higher-order solutions such as a five-velocity model, which is applicable to a regular lattice because the ratio $|r_{2,3}/r_{4,5}|$ is rational (3) in Eqs. (16) and (17).

The problem is one-dimensional, and we take a lattice with 1000 points along the tube. The initial conditions are $C_L = \{N = p = 3,\ \theta = 1,\ u = 0\}$ for $Z < 500$ and $C_R = \{N = p = \theta = 1,\ u = 0\}$ for $Z \geqslant 500$. The boundary conditions are C_L at $Z = 1$ and C_R at $Z = 1000$. We used $\tau = 1$ for the relaxation time of Eq. (1). If we decrease τ, the viscosity increases in the flow and the gradients of the physical quantities decrease. We show the normalized pressure profiles with respect to the variation of τ in Fig. 2.

Our result shows clearly a shock wave on the right side and an expansion wave on the left side for density, pressure, temperature, and velocity. Moreover, between the shock and the expansion waves, a discontinuity of temperature and a constant pressure are shown. We remark that a peak appears on the summit of the velocity profile, which is not expected from the Euler equations. The height of the peak decreases as time passes. The physical values of the simulation result are well matched with those obtained by solution of the Euler equations. We can convert the normalized velocity to the real velocity via $U = \sqrt{\Theta_0}u = \sqrt{2kT_0/m}u$. The speed of the shock wave is about 100 m/s at room temperature for

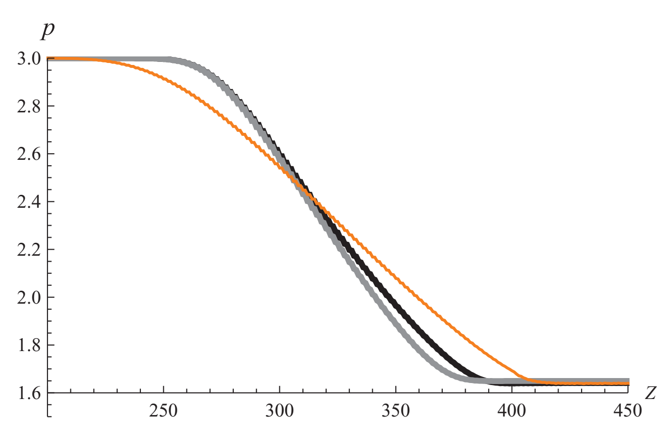

FIG. 2. (Color online) Normalized pressure profiles in the expansion shock wave region with respect to the variation of $\tau = 1$ (thick black line), $\tau = 0.5$ (thick gray line), and $\tau = 0.3$ (thin orange line) after 100 time steps. The vertical axis label p represents the normalized pressure and the horizontal axis label Z represents the location number.

TABLE I. Comparison of plateau values in profiles of density, pressure, temperature, and velocity between analytical solution of Riemann problem and our TLBM simulation obtained by one-dimensional five-velocity model.

Physical property	Normalized distance from the left end	Analytical solution	TLBM simulation
Density	z_1 (= 0.43)	2.46	2.43
	z_2 (= 0.65)	1.18	1.18
Pressure	z_2	1.65	1.64
Temperature	z_1	0.67	0.68
	z_2	1.40	1.39
Velocity	z_1	0.22	0.23
	z_2	0.22	0.22

nitrogen gas. The temperature jump in the shock wave is about 0.7 T_0, which is about 200 K at room temperature. Note that the simulation result of Chikatamarla and Karlin [5,6] shows only the density distribution of the *isothermal* problem. Moreover, the density distribution has three steps in their simulation result in contrast to the four steps in Sod's [21] and our results. However, our result shows the density, pressure, temperature, and velocity distributions of the *thermal* problem, and the results are consistent with the solutions having four steps of the density distribution obtained by the Euler equations.

We compare our simulation result for the one-dimensional five-velocity model to the analytical solution of the Riemann problem [22] in Table I. They are in good agreement; the differences are less than 1.63% which occurs at the normalized distance 0.43 from the left end for the density.

IV. CONCLUSION

We conclude this paper. We proposed a framework to derive the TLBM and derived a one-dimensional five-velocity and a two-dimensional 13-velocity model. The framework is based on the TE in variables of *temperature as well as velocity* and a direct calculation based upon the Gaussian quadrature hypothesis. It is possible to enhance the accuracy of the LBM and TLBM models by obtaining a higher-order TE and increasing the number of discrete velocities. Our framework provides higher-order models which are eventually more accurate in a regular lattice. Also, it provides the extension to thermal models in the same framework. The simulation of the one-dimensional shock tube problem shows that our model is also stable.

ACKNOWLEDGMENTS

This work was partially supported by the KIST Institutional Program.

[1] P. L. Bhatnagar, E. P. Gross, and M. Krook, Phys. Rev. **94**, 511 (1954).
[2] Y. H. Qian, D. D'Humières, and P. Lallemand, Europhys. Lett. **17**, 479 (1992).
[3] H. Chen, S. Chen, and W. H. Matthaeus, Phys. Rev. A **45**, R5339 (1992).
[4] X. He and L.-S. Luo, Phys. Rev. E **56**, 6811 (1997).
[5] S. S. Chikatamarla and I. V. Karlin, Phys. Rev. Lett. **97**, 190601 (2006).
[6] S. S. Chikatamarla and I. V. Karlin, Phys. Rev. E **79**, 046701 (2009).
[7] G. McNamara and B. Alder, Physica A **194**, 218 (1993).
[8] F. J. Alexander, S. Chen, and J. D. Sterling, Phys. Rev. E **47**, R2249 (1993).
[9] Y. Chen, H. Ohashi, and M. Akiyama, Phys. Rev. E **50**, 2776 (1994).
[10] X. He, S. Chen, and G. D. Doolen, J. Comput. Phys. **146**, 282 (1998).
[11] N. I. Prasianakis and I. V. Karlin, Phys. Rev. E **76**, 016702 (2007).
[12] S. Ansumali and I. V. Karlin, Phys. Rev. Lett. **95**, 260605 (2005).
[13] X. Shan, X.-F. Yuan, and H. Chen, J. Fluid Mech. **550**, 413 (2006).
[14] P. C. Philippi, L. A. Hegele Jr., L. O. E. dos Santos, and R. Surmas, Phys. Rev. E **73**, 056702 (2006).
[15] D. N. Siebert, L. A. Hegele Jr., and P. C. Philippi, Phys. Rev. E **77**, 026707 (2008).
[16] S. Chen and G. D. Doolen, Annu. Rev. Fluid. Mech. **30**, 329 (1998).
[17] *Handbook of Mathematical Functions with Formulas, Graphs, and Mathematical Tables*, edited by M. Abramowitz and I. A. Stegun (Dover, New York, 1972), p. 890.
[18] J. W. Shim, Ph.D. thesis, Université Pierre et Marie Curie (Paris VI), 2008.
[19] J. W. Shim and R. Gatignol, *La Houille Blanche*, Int. Water J. **5**, 120 (2009).
[20] P. Pavlo, G. Vahala, and L. Vahala, Phys. Rev. Lett. **80**, 18 (1998).
[21] G. A. Sod, J. Comput. Phys. **27,** 1 (1978).
[22] R. Courant and K. O. Friedrichs, *Supersonic Flow and Shock Waves* (Springer, New York, 1976), p.181.